Interference effects in the sum frequency generation spectra of thin organic films. II: Applications to different thin-film systems

Yujin Tong (仝玉进),[1] Yanbao Zhao (赵彦保),[1] Na Li (李娜),[1] Yunsheng Ma (马运生),[1] Masatoshi Osawa (大澤雅俊),[1] Paul B. Davies,[2,a)] and Shen Ye (叶深)[1,3,b)]
[1]*Catalysis Research Center, Hokkaido University, Sapporo 001-0021, Japan*
[2]*Department of Chemistry, University of Cambridge, Lensfield Road, Cambridge CB2 1EW, United Kingdom*
[3]*PRESTO, Japan Science and Technology Agency (JST), Tokyo, Japan*

(Received 28 January 2010; accepted 15 April 2010; published online 16 July 2010)

In this paper, the results of the modeling calculations carried out for predicting the interference effects expected in the sum frequency generation (SFG) spectra of a specific thin-layer system, described in the accompanying paper, are tested by comparing them with the experimental spectra obtained for a real thin-layer film comprising an organic monolayer/variable thickness dielectric layer/gold substrate. In this system, two contributions to the SFG spectra arise, a resonant contribution from the organic film and a nonresonant contribution from the gold substrate. The modeling calculations are in excellent agreement with the experimental spectra over a wide range of thicknesses and for different polarization combinations. The introduction of another resonant monolayer adjacent to the gold substrate and with the molecules having a reverse orientation has a significant affect on the spectral shapes which is predicted. If a dielectric substrate such as CaF_2 is used instead of a gold substrate, only the spectral intensities vary with the film thickness but not the spectral shapes. The counterpropagating beam geometry will change both the thickness dependent spectral shapes and the intensity of different vibrational modes in comparison with a copropagating geometry. The influences of these experimental factors, i.e., the molecular orientational structure in the thin film, the nature of the substrate, and the selected incident beam geometry, on the experimental SFG spectra are quantitatively predicted by the calculations. The thickness effects on the signals from a SFG active monolayer contained in a thin liquid-layer cell of the type frequently used for *in situ* electrochemical measurements is also discussed. The modeling calculation is also valid for application to other thin-film systems comprising more than two resonant SFG active interfaces by appropriate choice of optical geometries and relevant optical properties. © *2010 American Institute of Physics*. [doi:10.1063/1.3428673]

I. INTRODUCTION

In the preceding paper, we reported the theoretical modeling and simulation of the thickness-induced interference effect on sum frequency generation (SFG) signals from a thin-layer system consisting of a fatty acid monolayer on a dielectric thin film deposited on a gold substrate.[1] By taking multiple reflections and phase differences between the signals from the two interfaces into account, we formulated a model which quantitatively accounts for the interference effect in the thin-layer system. The simulation demonstrates that the line shape and intensity of the SFG spectra are significantly dependent on the thickness of the dielectric thin film for different polarization combinations.

In the present paper, the simulated results are compared with the experimental observations to test the validity of the model. We compare the observed SFG spectra of the thin-layer model system used in the preceding paper,[1] prepared experimentally by the Langmuir–Blodgett (LB) method with the simulation prediction. Thereafter, we further extend the model calculation to several different thin-layer systems which have been experimentally probed by SFG. The influence of different experimental parameters, such as the incident beam geometry (copropagating and counterpropagating), substrate (metal and dielectric materials), and thin-film structures on the SFG spectra is discussed by comparing the simulations with the observations. Finally, the thin solution layer system, which is widely used in *in situ* electrochemical spectroscopy, is also discussed in the context of the model calculation.

II. EXPERIMENTAL

The model thin-film system used in the preceding paper (Fig. 2 in Ref. 1) has been constructed experimentally. LB multilayers have been extensively employed as standard model systems for experiments[2–4] and for theoretical simulations.[5–7] In our experiments, dielectric films comprising Y-type multilayers of per-deuterated arachidate with various thicknesses (4–80 layers) were deposited on gold substrates followed by the deposition of a monolayer of per-protonated arachidate on the top surface, as depicted schematically in Fig. 1. In this case, the SFG resonant signals

a)Electronic mail: pbd2@cam.ac.uk.
b)Electronic mail: ye@cat.hokudai.ac.jp.

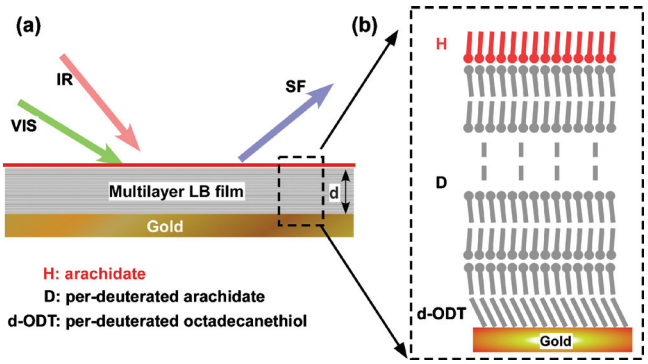

FIG. 1. Schematic diagrams of the multilayer LB film on a gold substrate.

in the C–H stretching region originate only from the topmost, free air/film interface, while the "per-deuterated" dielectric film does not produce any contributions in the C–H region and hence works as a buffer or dielectric layer. The SFG signals from the buried film/gold interface in the same frequency region are solely due to the nonresonant SFG signal from the gold substrate. Recently, Lagutchev *et al.* reported that the nonresonant background signal from the gold substrate in broadband SFG measurements can be significantly reduced by introducing a time delay between the IR and visible pulses.[8] When the per-deuterated dielectric thin film is replaced by a per-protonated one, the resonance signal will come from both interfaces, in which case the model is modified by including the contribution of the resonant C–H signal from the buried interface (see below). No resonant SFG signal will be generated from the bulk of this multilayer film due to its centrosymmetric structure.

In order to keep the gold surface reproducible for the LB preparation, freshly evaporated gold films (ca. 200 nm thick) on glass slides were immersed in a 1 mM methanol solution of per-deuterated octadecanethiol (d-ODT) for 12 h at room temperature to form a self-assembled monolayer (SAM) on the gold surface. The gold surface becomes completely hydrophobic after formation of the d-ODT SAM. The hydrophobic gold substrate is stable in air and is used for LB film deposition as follows. Monolayers of the per-deuterated or per-protonated arachidic acid (Cambridge Isotope Laboratories, Inc.) were prepared at the subphase/air interface by spreading chloroform solutions of the fatty acid molecule (1.00 mg/mL) onto an LB trough (FSD-500, USI System, Japan) containing a subphase of cadmium chloride (0.2 mM) and sodium hydrogen carbonate (0.3 mM) in Milli-Q water (pH 6.6). Following chloroform evaporation, the films were compressed to a surface pressure of 30 mN/m and allowed to equilibrate for 30 min. The Y-type LB multilayers of the per-deuterated arachidate [Fig. 1(b)] with different layer thicknesses (4, 10, 20, 30, 40, 50, 60, 70, and 80 monolayers) except for the top-monolayer of the per-protonated arachidate, were deposited by sequential vertical dipping of the hydrophobic gold substrate. The layer thickness of the per-deuterated arachidate bilayer was estimated to be 5.7 ± 0.1 nm/bilayer based on the results obtained by ellipsometry[5] and grazing incidence x-ray diffraction.[9] The thickness of a multilayer is determined by adding together the thickness of the d-ODT monolayer (2.5 ± 0.1 nm),[10] per-deuterated LB-multilayer and topmost per-protonated monolayer.

The SFG spectra were recorded in the C–H stretching region (2800–3000 cm^{-1}) by a broadband femtosecond SFG spectrometer consisting of a Ti:sapphire femtosecond oscillator/regenerative amplifier laser system (Spitfire, Spectra Physics, 100 fs, 2.25 mJ, 800 nm, 1 kHz). About 50% of the laser output was used to pump an optical parametric amplifier system (TOPAS, Light Conversion, Inc.) to generate a broadband tunable IR beam (ca. 200 cm^{-1}). The remainder of the broadband visible output at 800 nm was converted to a *ps* pulse tunable from the UV to near IR region (220–1000 nm) by a TOPAS-white-NB. The *ps* visible pulse at 800 nm can also be generated by a homemade spectral shaper,[2] which was the device actually used in the present study. The visible and infrared beams overlapped on the substrate with incident angles of 70° and 50°, respectively, in a copropagating beam geometry. The SFG signal was dispersed through a monochromator (MS3501i, Solar-TII) and collected by a CCD camera (DU420-BV, Andor Technology).

The SFG spectra were recorded in *ppp*, *ssp*, and *sps* polarization combinations. The *ppp* polarization SFG spectra were accumulated for 1 min. Longer acquisition times were used for the *ssp* and *sps* polarizations due to their lower SFG intensities. Depending on the film thickness, the acquisition time was typically shorter than 10 min (*ssp*) and 30 min (*sps*). The intensities of the SFG spectra were normalized by an SFG spectrum from a d-ODT modified gold substrate and the acquisition time.

III. RESULTS AND DISCUSSION

A. Monolayer/dielectric film/gold substrate system

In order to test the validity of the theoretical modeling presented in Ref. 1, SFG characterizations were carried out using the LB multilayer system shown in Fig. 1 with various thicknesses of the per-deuterated arachidate LB film and a top monolayer of per-protonated arachidate. The number of layers, n=4, 10, 20, 30, 40, 50, 60, 70, and 80, correspond to thicknesses (d) of 14, 30, 59, 87, 116, 144, 172, 200, and 230 nm, respectively.[11] The simulations were conducted for the model system investigated in a previous paper[1] using the refractive index of a multilayer film of fatty acid for the dielectric thin film. The experimentally observed *ssp*, *sps*, and *ppp* polarized SFG spectra for the LB multilayer systems with various layer numbers are shown in Figs. 2(a), 2(c), and 2(e), respectively; while the corresponding simulated results are shown in Figs. 2(b), 2(d), and 2(f), respectively.

For the *ssp* polarization combination [Figs. 2(a) and 2(b)], the scale for each spectrum has been adjusted by the multiplication factor shown against each spectrum for clarity. When the number of LB layers are relatively low (n=4 and n=10), the spectra are dominated by two dips around 2878 and 2944 cm^{-1}, corresponding to the symmetric stretching (r^+) and Fermi resonant (r^+_{FR}) modes, respectively, of the methyl (CH_3) groups in the top monolayer of the per-protonated

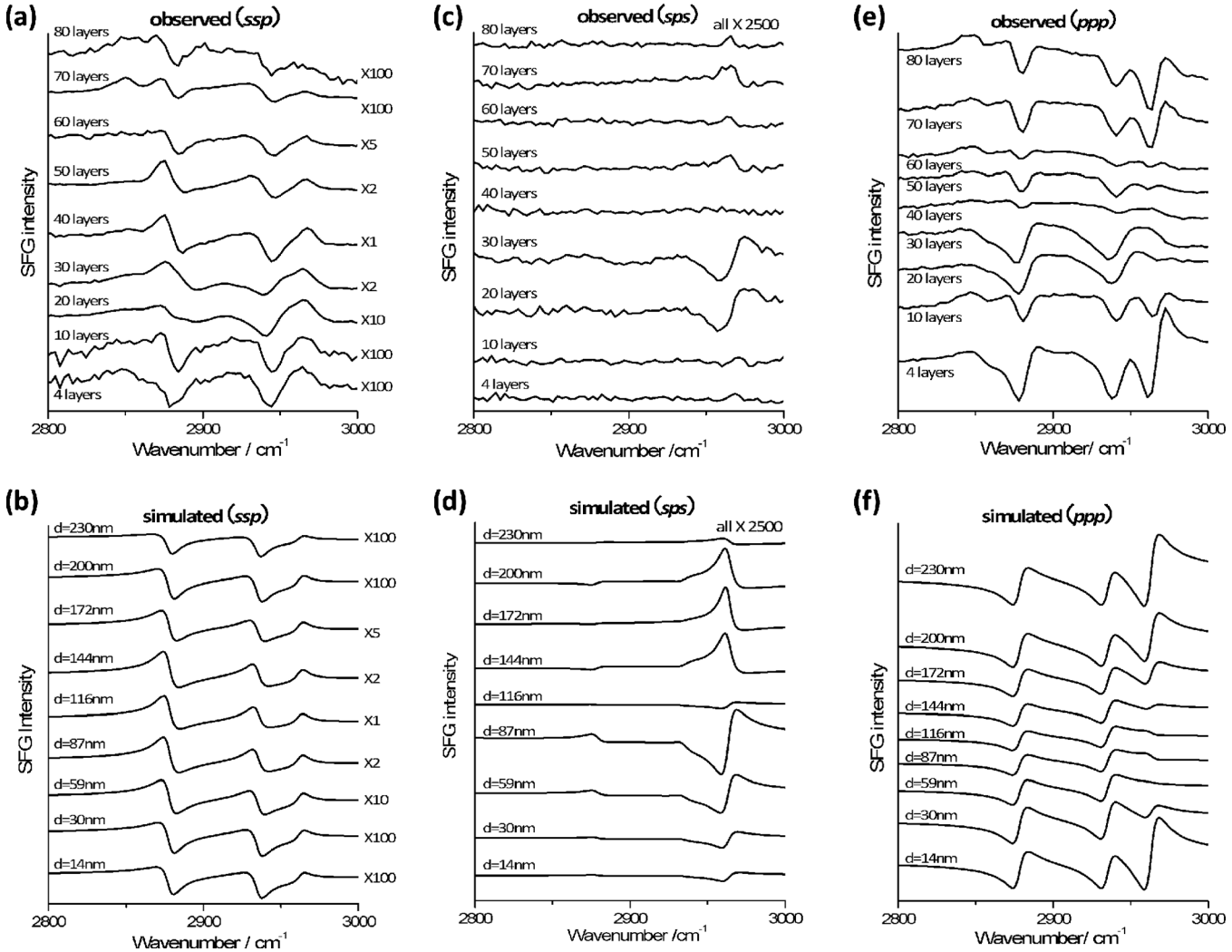

FIG. 2. Experimentally observed [(a), (c), and (e)] and simulated [(b), (d), and (f)] SFG spectra of multilayer LB films for the different polarization combinations of *ssp* [(a) and (b)]; *sps* [(c) and (d)], and *ppp* [(e) and (f)] with different film thicknesses. From bottom to top, n=4, 10, 20, 30, 40, 50, 60, 70, and 80 (number does not include the d-ODT monolayer) corresponding to thicknesses of d=14, 30, 59, 87, 116, 144, 172, 200, and 230 nm, for observed and simulated results, respectively. For comparison purposes, the scale for each spectrum of [(a) and (b)] has been adjusted by the multiplication factor shown next to the spectrum. The spectra are offset for clarity.

arachidate. Additionally, a peak can be observed at 2964 cm^{-1}, attributed to the asymmetric stretching mode (r^-) of the CH_3 group. The S/N ratios for the SFG spectra of the four and ten layers are low due to the very weak SFG signals at these thicknesses. The shape of the SFG spectra is similar to those reported previously for SAMs on a gold surface.[12,13] The spectral intensities rapidly increase when the number of LB layers is increased beyond 10. The spectral intensities at n=20, 30, and 40 layers are approximately 10, 50, and 100 times higher than those for n=4. At the same time, the spectral profiles for the r^+ and r^+_{FR} modes display "Z"-shaped bipolar features. The r^- mode retains a peak shape while its intensity changes significantly with the film thickness. The spectral intensities start to decrease as the number of LB layers becomes greater than 40. For example, the spectral intensities at n=50 and n=60 are about half and one fifth of those at n=40. As the thickness is further increased, the SFG spectrum becomes similar to that for n=4. As shown in Fig. 2(a), the spectra at n=70 and 80 mainly show two weak dips around 2878 and 2944 cm^{-1}, resembling those at n=4. Note that the symmetric (d^+) and asymmetric (d^-) C–H stretching modes of the methylene (CH_2) groups, arising from the *gauche* defects in the layers,[14–17] can also be observed around 2850 and 2920 cm^{-1}, respectively. These film defects sometimes appear in the LB multilayers during film deposition and their extent is not experimentally controllable. The influence of the *gauche* defects on the SFG signals becomes greater with increasing thickness of the LB multilayers (see below).

Figure 2(b) shows the simulated *ssp*-spectra for the same multilayer systems. The simulated results are shown with the same magnification as that for the experimental observations at the same thickness. A comparison of the two shows that the simulations accurately reproduce the spectral intensities and profiles for the multilayer systems. For example, both simulation and experiment show that the spectral intensities change by two orders of magnitude for different film thicknesses. Moreover, the weak dips observed for thinner layers (14 and 30 nm) change to strong bipolar peaks (59, 87, 116, 144, and 172 nm) and back to the weak dips for the thicker

films at 200 and 230 nm. These results amply demonstrate the validity of the simulations. Although it might be expected that the monolayer of the per-protonated arachidate deposited on the surface of the per-deuterated arachidate multilayers of different thicknesses on a gold substrate surface should have the same structure regardless of layer thickness, the SFG spectra show very different spectral intensities and shapes. As discussed in detail in the preceding paper,[1] these thickness-dependent features are due to interference between the resonant and the nonresonant signals from the free and buried interfaces in the thin-film structure (Fig. 1). In the present simulation, methylene resonances, i.e., *gauche* defects as mentioned above, have not been considered in the modeling although one can expect the interference will also strongly affect the appearance of the SFG resonance that arises from the defects.

The observed SFG spectra in the *sps* polarization [Fig. 2(c)] are much weaker than those in the *ssp*-polarization. All the *sps*-spectra shown in Fig. 2(c) are magnified 2500 times for comparison purposes. As shown in Fig. 2(c), the spectral intensities of the *sps*-spectra for $n<20$ are too weak to be observed. However, as the layer number increases, for example, from n=20 to 30 [Fig. 2(c)], some "S"-type bipolar peaks for the r^- mode around 2957 cm^{-1} are clearly discernable but the signal almost disappears by n=40. As the number of LB layers is further increased, the SFG signal appears again, but this time showing Z-type bipolar features as shown in the spectra at n=50, 60, and 70. The SFG signals decrease again as the layer number reaches 80. It is worth noting that to the authors' knowledge, no SFG results on a gold substrate under *sps*-polarization have been published before due to the weak signal level. The present experiment convincingly demonstrates that if a suitable thickness of thin film on the gold surface is used, it is possible to get reasonably strong *sps*-SFG signals by exploiting the interference effect.

Figure 2(d) shows the simulated *sps*-spectra for the multilayer systems. The simulations again accurately reproduce the observed spectral features. For example, the spectral line shape changes from an S-type bipolar shape to a Z-like bipolar shape as the multilayer thickness passes through 116 nm. As described in the previous paper, the switching of the spectral features in this way can be ascribed to the change in the relative phase of the resonant and the nonresonant contributions.

Figure 2(e) shows the observed *ppp*-spectra. The *ppp*-spectra are dominated by three peaks around 2878, 2937, and 2960 cm^{-1}, corresponding to the r^+, r^+_{FR}, and r^- vibrational modes. Most of these spectra are also affected by the d^+ (ca. 2850 cm^{-1}) and d^- (2920 cm^{-1}) modes from the *gauche* defects in the films. The *ppp*-SFG spectrum at n=4 is similar to that of a fatty acid monolayer reported previously.[2,3,7] The interference phenomenon in the *ppp*-spectra is different from that in the *ssp*- and *sps*-spectra. The interference behavior is significantly dependent on the vibrational mode. The r^+ and r^+_{FR} modes show a dip in all the spectra on the present scale, while the shape of the r^- mode is significantly dependent on the film thickness. The S-shaped bipolar peak for the r^- mode at n=4 changes to a dip as the number of LB layers increases, then disappears completely at n=20. These features appear as tiny peaks again for n=30 and 40. The profile then changes to a dip again for n=50 and 60. Finally, the spectral profile of the r^- mode becomes similar to that at n=4 as the layer number becomes greater than 60.

The simulated results shown in Fig. 2(f) accurately reproduce the observed spectral changes. From the analysis of the simulated features carried out in the preceding paper, these vibrational mode dependent interference features can be explained as follows: there are four susceptibility components for the *ppp* polarization combination and each has its own magnitude and sign and, in addition, the L factors for the different components are also different from each other. All these effects taken together determine the thickness-dependent interference effect for the *ppp* polarization combination.[18]

B. Organic thin film/gold substrate

The model discussed in Sec. III A (Fig. 1) and in the preceding paper[1] only dealt with the SFG spectra of a monolayer deposited on a dielectric thin film/gold substrate. This model system has the advantage of simplicity in which it is only necessary to consider the resonant C–H stretching contribution from the free air/film interface and the nonresonant contribution from the buried gold/film interface (Fig. 1). However, for other organic thin films such as a polymer thin film deposited on a substrate surface,[19–28] the buried interface may also contribute to the resonant SFG signals. The quantitative treatment of such a thin film is practically important and the model needs to be extended to these more general cases.

The calculation for such a thin film is identical to that above except for including an additional C–H resonant susceptibility from the buried interface and assuming that the CH_3 groups at the buried interface point toward the d-ODT modified Au substrate. Figure 3(a) shows schematically the structure of the LB multilayer this time using a per-protonated arachidic acid multilayer on a d-ODT SAM substrate. As previously reported,[5,6] there are two sources of resonant SFG here: one is located at the free air/multilayer interface, while the other is located at the buried multilayer/substrate interface [Fig. 3(a)]. The SFG signals from the layers in the middle of the LB multilayer cancel each other due to the centrosymmetric structure of the film. As has been reported previously,[6] the peak position of the methyl group from the bottom interface in the present simulation process is selected to be 3–5 cm^{-1} lower than that from the free air/film interface, due to their different environments.

Figures 3(b) and 3(c) show the observed and simulated *ssp*-polarized SFG spectra of a series of thin films [Fig. 3(a)] with a different number of layers (from bottom to top, n=2, 10, 20, 40, 50, 60, and 80, corresponding to thicknesses (d) of 8, 30, 59, 116, 144, 172, and 230 nm, respectively, including the d-ODT monolayer). In order to show these spectral profiles clearly, the scale for each spectrum has been adjusted

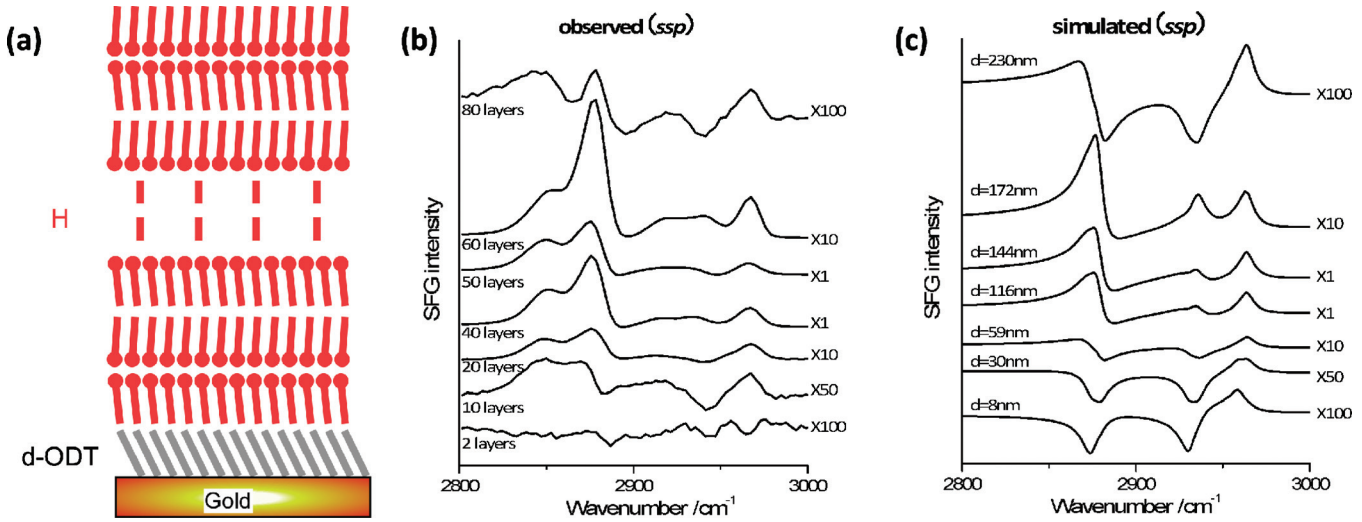

FIG. 3. (a) Schematic diagrams of the series of LB arachidic acid multilayers on a per-deuterated octadecanethiol modified gold substrate with all the layers per-protonated. [(b) and (c)] show the experimentally observed and simulated SFG spectra, respectively, of multilayer LB films for the *ssp* polarization combination with different film thicknesses. From bottom to top, n=2, 10, 20, 40, 50, 60, and 80 (number does not include the d-ODT monolayer) corresponding to thicknesses of d=8, 30, 59, 116, 144, 172, and 230 nm for the observed and simulated results, respectively. For comparison purposes, the scale for each spectrum of [(b) and (c)] has been adjusted by the multiplication factor shown next to the spectrum. The spectra are offset for clarity.

by a factor shown alongside each spectrum. Generally the simulation predicts most of the intensity and line shapes found in the experimental spectra. For example, the simulated SFG spectrum with n=60 is very similar to that for the observed SFG spectrum for a thickness of 172 nm and exhibits a strong peak shaped signal for all three resonances (i.e., for r^+, r^+_{FR} and r^-). As the film thickness increases, the SFG spectrum with n=80 (or d=230 nm) shows much weaker signals for all the resonances, with the r^+ and r^+_{FR} modes exhibiting a dip while r^- exhibits a peak shape. These results [Figs. 3(b) and 3(c)] also confirm the validity of the simulations. However, when compared to the spectra of Figs. 2(a) and 2(b) for the same thin-layer film thickness with a resonant source only from the free air/film interface, the observed SFG spectra [Fig. 3(b)] show significantly more *gauche* defect peaks. Since the present LB multilayer is constructed only from per-protonated molecules, all the individual layers may contain *gauche* defects generated during the film preparation process. These *gauche* defects will strongly affect the SFG spectral features due to the interference effect in the film. On the other hand, the SFG spectra in Fig. 3 show more complicated features compared to the spectra in Fig. 2. Most of the features in the SFG spectra in Fig. 3 have a bipolar shape, and additionally their positions also shift with the film thickness.[6] Nevertheless, it is interesting to note that the relative intensities of the spectra at the different film thicknesses in Fig. 3 seem to be comparable to those in Fig. 2, as emphasized by the multiplication factors shown beside the spectra. This is mainly due to the L factors for the two thin-film models [see Figs. 3(a) and 4(a) in the preceding paper[1]] being identical if the film thickness is the same. As has been extensively discussed in the preceding paper, the relative intensities are mainly determined by the L factors at a certain film thickness. Hence the intensities of the SFG spectra at the same film thickness for the two systems are comparable to each other. The only difference between the simulations shown in Figs. 2(a) and 3(a) are the susceptibility terms for the bottom interface [Eq. 12 in the preceding paper[1]]. The bipolar shapes themselves are due to the interference between the two resonant susceptibilities.

C. Effect of the Substrate

As many SFG characterizations have been carried out on thin-film samples deposited on dielectric substrates, such as CaF_2,[29,30] fused quartz,[31,32] and sapphire,[21,23,33] it would be interesting to know the differences in the interference effect for dielectric and metal substrates. Figure 4(a) shows a schematic structure for the same LB multilayer system as in Fig. 3(a) but where the hydrophobic gold substrate is replaced by a per-deuterated arachidate monolayer modified fused quartz one.

Simulated *ssp*-polarized SFG spectra for different film thicknesses of (from bottom to top) 0, 150, 300, 450, and 600 nm, are shown in Fig. 4(b). The intensity of the r^+ mode as a function of the film thickness is shown by the solid line in Fig. 4(c). Similar calculations were also carried out for the *sps*- and *ppp*-polarization combinations. Here, only the simulated results for the *ssp*-polarization are given. In comparison with the simulated results for the corresponding film systems on a gold substrate [Fig. 3(c)], several differences are observed. All the SFG resonant signals from the thin film on the dielectric substrate now appear as peaks rather than the dips or bipolar shapes which are observed on the gold surface [Figs. 2(b) and 3(c)]. The peak intensities change significantly in magnitude with the film thickness. This phenomenon can be attributed to the negligible nonresonant susceptibility $\chi^{(2)}_{NR}$ from the fused quartz substrate compared to the gold substrate.[6] As pointed out in the theoretical part of the preceding paper,[1] if the nonresonant susceptibility is much smaller than the resonant contribution, the buried interface will only contain a resonant contribution. The two resonant terms from the two interfaces interfere with each other and affect only the intensity and not the peak shapes. It

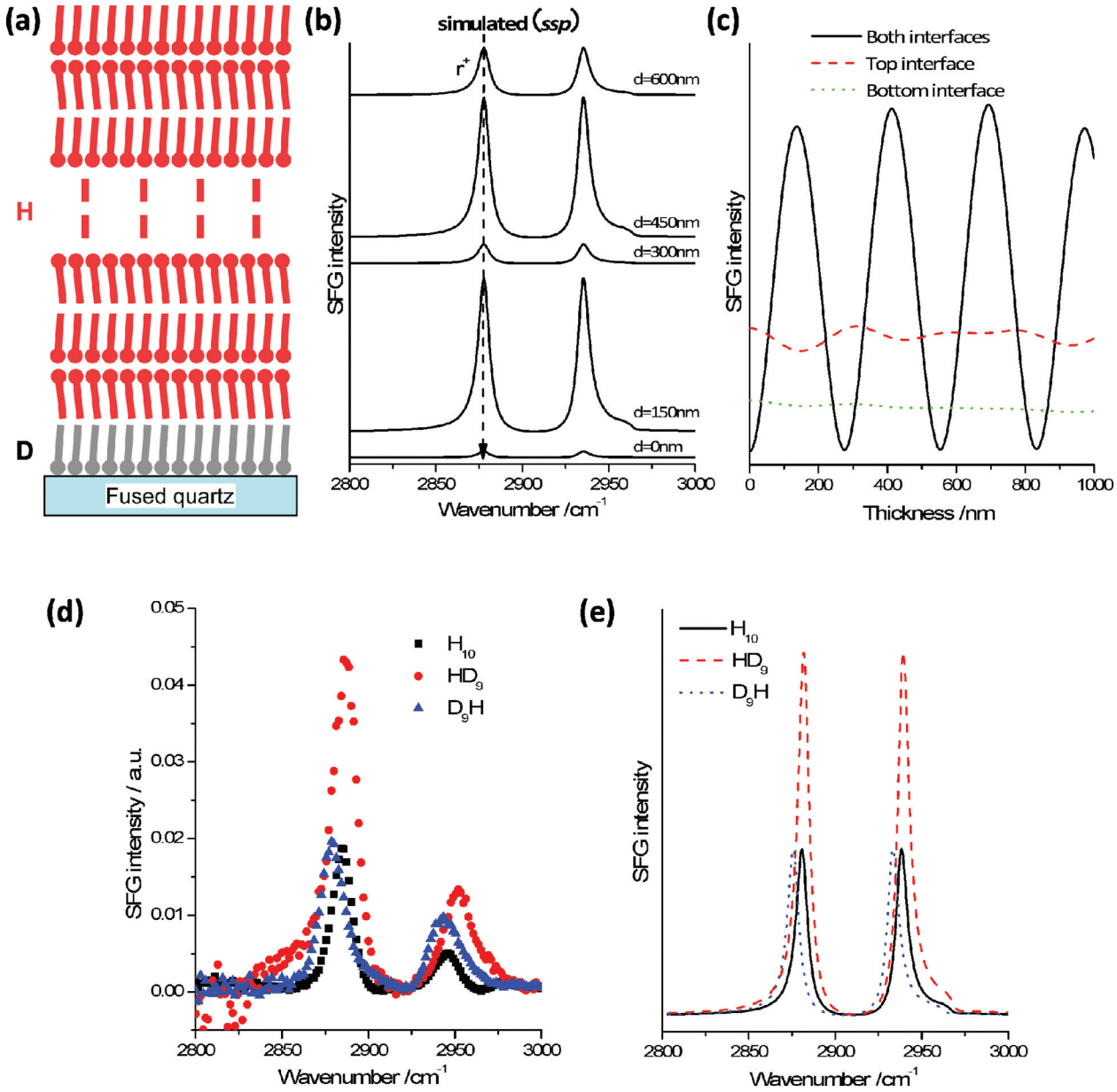

FIG. 4. (a) Schematic diagram of the LB multilayer thin film on a dielectric substrate. (b) Simulated SFG spectra of the model thin film of Fig. 4(a) for different thin-film thicknesses: from bottom to top, 0, 150, 300, 450, and 600 nm for the *ssp* polarization combination. (c) SFG intensities at the r^+ mode peak position from both interfaces (solid line), from the air/thin-film interface only (dashed line) and from the thin film/substrate interface only (dotted line) as a function of the thin-film thickness. (d) Observed SFG spectra for a ten layer per-protonated cadmium arachidate multilayer film (denoted as H_{10}, solid line), a nine-layer per-deuterated cadmium arachidate film with a per-protonated topmost layer (denoted as HD_9, dashed line), and a nine-layer per-deuterated cadmium arachidate film with a per-protonated lowermost layer (denoted as D_9H, dotted line). All films were deposited on per-deuterated cadmium arachidate monolayer modified fused quartz as described in Sec. II. (e) Corresponding simulated SFG spectra at d=55 nm for the multilayer system of Fig. 4(d). Base line levels for each spectrum in (b) are displaced for clarity.

is then necessary to separate the contributions from the interfaces to determine the SFG spectrum at each interface. The dashed and solid lines of Fig. 4(c) represent the peak intensities of the r^+ mode SFG signals from the free air/film and buried film/substrate interfaces. Clearly, the signal from the free interface is larger than that from the buried interface. This result indicates that separating the interference effects from the two interfaces enables the molecular structures at each interface of a thin film to be determined.

As an example, Figs. 4(d) and 4(e) show the observed and simulated SFG spectra, respectively, for a ten layer per-protonated cadmium arachidate multilayer film [denoted as H_{10}, square symbol in Fig. 4(d) and solid line in Fig. 4(e)], nine-layer per-deuterated cadmium arachidate film with a per-protonated topmost layer [denoted as HD_9, circular symbols in Fig. 4(d) and dashed line in Fig. 4(e)], and nine-layer per-deuterated cadmium arachidate film with a per-protonated lowermost layer [denoted as D_9H, triangular symbol in Fig. 4(d) and dotted line in Fig. 4(e)] on a per-deuterated arachidate monolayer modified fused quartz substrate as described in Sec. II. All three films are 55 nm.

The experimental observations [Fig. 4(d)] show that for the r^+ mode, the SFG intensity from the top free interface (HD_9) is stronger than that from the buried interface (D_9H),

which is consistent with the simulations shown in Fig. 4(c). Moreover, for the actual film thickness of about 55 nm, the intensity of the SFG signal contributed from both the free and buried interfaces (H_{10}) is comparable to that arising from the buried interface, but only half of that arising from the free interface. It is also noted that a distinct red shift in the resonance frequencies exists when comparing these spectra. The shift corresponds to a change in the local environment of the methyl groups as has been extensively discussed in a previous paper.[6] The main features of the experimental results [Fig. 4(d)] are well reproduced in the simulation [Fig. 4(e)], further confirming the validity of the modeling simulations.

The present model system can be applied to a thin polymer film deposited on a dielectric substrate by appropriately changing the parameters in the model simulation. As shown in Fig. 4, the SFG signals from both interfaces as well as the interference between them will contribute strongly to the observed SFG spectrum. By elucidating the exact spectrum at each interface, it becomes possible to analyze the molecular structures at each interface, which is essential for an exact analysis of the overall SFG spectra from the thin-film surface.

D. Effect of incident beam geometry

The incident laser beam geometry in SFG experiments can be either co- or counterpropagating. The counterpropagating geometry was frequently adopted[6,15,34–36] in the initial development of SFG. The counterpropagating system has the advantage that the angle between the reflected SFG light and the reflected visible pump beam is greater than that for the copropagating geometry, which reduces the influence of the scattered visible light and aids more efficient collection of the SFG light.[6,15,34–36] This geometry is also used in pump-probe experiments since it can use the experimental space in an efficient way.[34] Recently, the copropagating geometry has become more widely used due to its simplicity for alignment and maintenance. Since the L factors for the copropagating and counterpropagating geometries are different, it is not straight forward to make a direct comparison of the SFG spectra obtained with the different geometries. On the other hand, many valuable experiments and calculations have also been carried out using the counterpropagating arrangement.[35,37,38] In order to compare and discuss these studies, we need an intercomparison of the experiments and calculations obtained for the two geometries.

The thin-film model with the counterpropagating geometry is shown in Fig. 5(a), in which a thin dielectric layer is sandwiched between air and a gold substrate with a monolayer of arachidic acid adsorbed on the top of the thin dielectric layer. In comparison to the systems shown in Fig. 1, there are several differences to be considered in the calculations for the two geometries, namely,

(1) *The relative phase difference between the resonant and nonresonant susceptibilities.*[6,13,36]
(2) *The angle of the emitted SFG beam.* According to the laws of conservation of energy and momentum, the angle of the emitted SFG beam in the counterpropagating geometry is smaller than that in the copropagating geometry, if the incident beam angles are the same. This will cause a shorter periodicity for the multiple reflection of the SFG beam in the thin film, and further affects the interference behavior.
(3) *The additional phase of Eq. 11 given in the preceding paper.*[1] The equations used to calculate the additional phase will be different from those given in Eq. 11 in the preceding paper. The expression for the additional phase for the counterpropagating incident beam geometry has been reported elsewhere,[18,19] and will not be reproduced here.
(4) *The expression for the final SFG intensity given in Eq. 12 in the preceding paper for the ppp polarization changes.* As the IR electric field along the x Cartesian axis in the counterpropagating geometry is opposite to that in the copropagating geometry, all the x components of the IR electric field in Eq. 12 must change in sign. Consequently, the signs of the second, third, sixth and seventh terms of Eq. 12-iii need to be exchanged.[1]

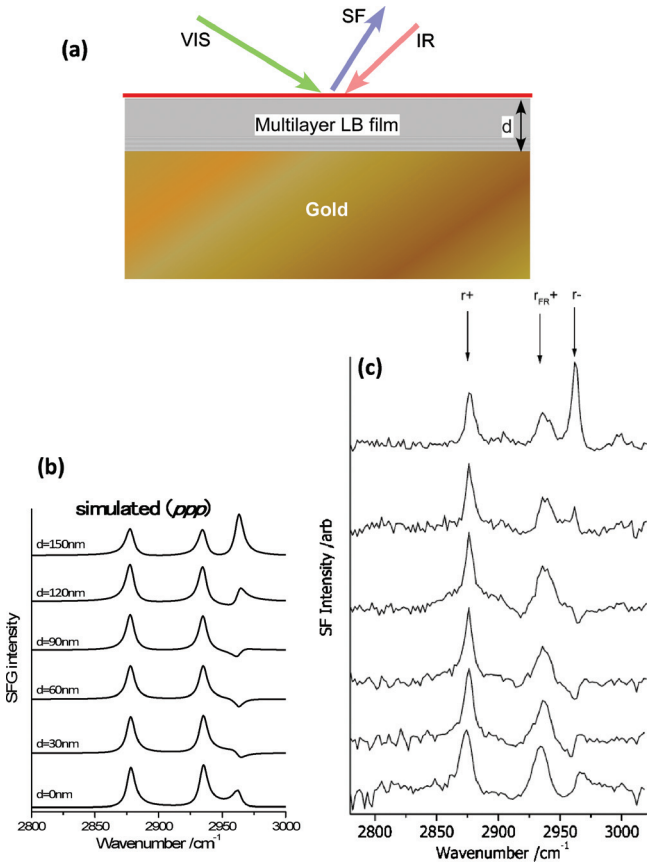

FIG. 5. (a) Schematic diagram of the thin-layer system using a counterpropagating incident beam geometry. (b) Simulated SFG spectra of the model thin film for various film thicknesses: from bottom to top, 0, 30, 60, 90, and 120 nm with the *ppp* polarization combination. Baseline levels for each spectrum are displaced for clarity. (c) Corresponding experimental result for the SFG spectra obtained from an LB multilayer arachidic acid film on a gold substrate with the topmost layer of each film per-protonated and all the lower layers per-deuterated: from bottom to top with, 2, 10, 20, 30, 40, 50, and 60 layers. Reproduced from Fig. 7 of Ref. 5

In order to check the feasibility of the application of the calculation model for the counterpropagating geometry, we

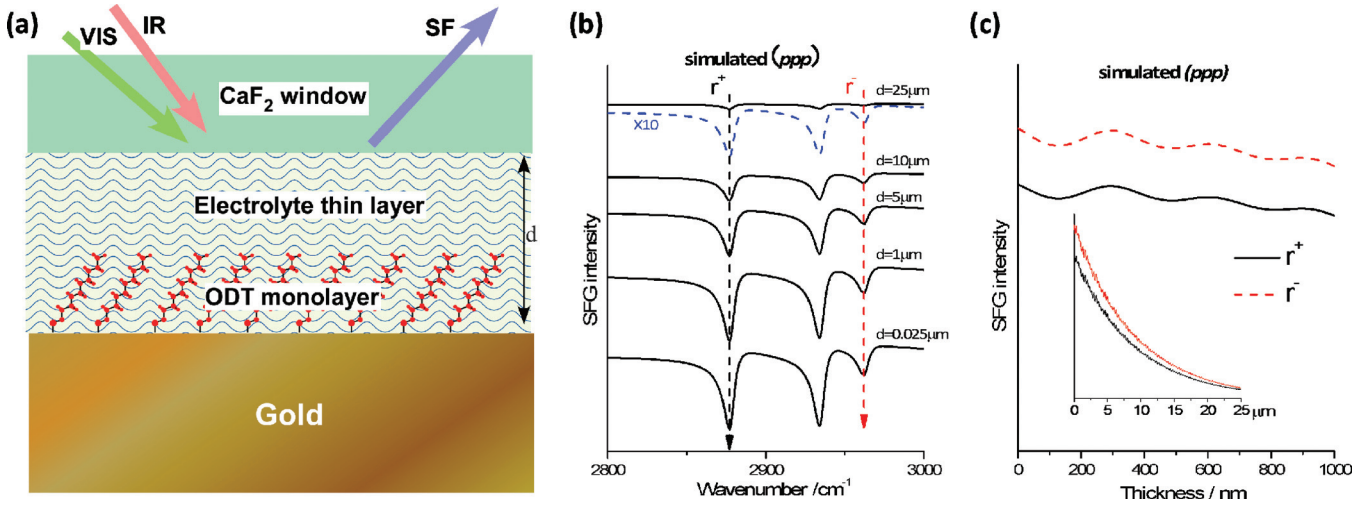

FIG. 6. (a) Schematic diagram of the air/CaF_2 window/electrolyte thin layer/ODT monolayer/gold electrode thin-layer system. (b) Simulated results for *ppp*-polarized SFG spectra with various thicknesses of the electrolyte thin layer (the spectra with d=25 μm magnified ten times is also shown for comparison) and (c) SFG intensities at the indicated peak position as a function of the thin-layer thickness. The SFG peak intensity changes over the thickness range of 0–25 μm is shown as an inset in (c). Baselines for each spectrum in (b) have been displaced for clarity.

have also simulated the SFG spectra [Fig. 5(b)] under the counterpropagating geometry and compared this simulation with previous observations reported by the Cambridge group [Fig. 5(c)]. As shown, the simulation results agree well with the experimental observations.[4] For example, our calculation shows that the intensity of the r^+ mode will only change slightly with the film thickness, while that of the r^- mode will change from peak (d=0) to dip (d=60 nm) and finally become a peak again at d=150 nm. The experimental results confirm these predications. Moreover, our simulations also predict the relative peak intensities. As shown in Figs. 5(b) and 5(c), as the thickness increases to 150 nm, the asymmetric peak becomes stronger than the symmetric peaks. This behavior is clearly observed in the experimental results. As described in the preceding paper, the relative intensity change in the different modes at distinct film thicknesses is due to the different contribution of the four terms in Eq. 12-iii of the preceding paper. In comparison with the modeling results proposed by Lambert *et al.*,[18] the present simulation can either exactly predict the line shape of the peaks or give the relative intensity of each peak. As discussed in the preceding paper, when there are several contributions to the interference phenomenon it should be noted that periodic changes in the spectral features do not exist due to the complicated nature of the overall interference as shown above.

E. Electrochemically active thin-layer system

As mentioned in Sec. I, *in situ* SFG observations have been carried out for electrochemical systems.[39–44] In this case, in order to reduce the IR absorption by the aqueous electrolyte solution, a thin-layer geometry has usually been employed in which the electrode is usually placed on an optical window (usually, CaF_2 or BaF_2 is used) to form a thin solution layer estimated to be several microns thick. Since it is not possible to control the thickness of the thin layer exactly, it is necessary to consider the possibility of interference in the thin layer of electrolyte solution contained between the electrode and the optical window. In this section, the model simulation on a thin-layer system at an electrode/solution interface will be examined. The model is shown in Fig. 6(a), where a thin layer of aqueous electrolyte solution (ca. tens of microns in thickness) is sandwiched between a CaF_2 window and a gold electrode modified by a well-ordered ODT monolayer. SFG measurements are conducted by shining the visible and IR beams from the window side, and detecting the SFG signal in the reflection mode.

Figures 6(b) and 6(c) show the simulated *ppp*-polarized SFG spectra at several thicknesses and the resonant peak intensity for the r^+ and r^- modes, respectively, as a function of film thickness. The spectral shapes are quite similar between d=0 and 25 μm while the spectral intensities change significantly [Figs. 6(b) and 6(c)]. The spectrum for the monolayer case [d=2.5 nm, bottom spectrum of Fig. 6(b)] shows a shape similar to those reported by Zhang *et al.*[13] for an analogous system. As shown in Fig. 6(b), the SFG spectral shape of the ODT monolayer on a gold electrode surface seems to be independent of the thickness of the thin solution layer, while the intensity significantly decreases with the thickness of the layer. As discussed in the preceding paper, the thickness dependent spectral line shapes only occur when the relative intensity or phase or both change with the film thickness. In the present aqueous thin layer for the *in situ* electrochemical SFG measurement, the change in the thin layer will affect neither the relative intensity nor the relative phase, since both the resonant sources (ODT monolayer) and the nonresonant source (gold electrode) are from the same interface. Hence, no thickness dependent spectral line shape should be observed. In fact, this prediction concurs with the reported results even though the thickness of the thin solution layer cannot be accurately controlled, and the spectral line shapes obtained from different groups for the same sample were similar to each other.[39–44]

On the other hand, the intensity of the SFG signal for different film thicknesses exhibits some thickness dependent features. For example, Fig. 6(c) indicates that over a short range of hundreds of nm, the SFG signals oscillate signifi-

cantly with the film thickness. When the thickness is extended to tens of microns, an exponential decay in the SFG signal is observed, which is due to the strong absorption of the IR beam by the electrolyte solution in the thin layer.

From these results it is concluded that, when the SFG/electrochemical thin-layer system is measured, the features of an SFG spectrum arising from a monolayer on an electrode surface is almost independent of the thickness of the aqueous layer. On the other hand the thinner the electrolyte layer the stronger the SFG signals. If the film is too thin, serious problems in potential control and mass transfer can arise, and hence there is a need to choose the optimum thickness for acceptable SFG signal intensity and effective electrochemical controls.

IV. CONCLUSION

In the present paper model calculations were first validated by comparing the experimental observations and the simulation results obtained for a model multilayer LB film. The SFG spectral intensities and shapes for a system consisting of an organic monolayer separated from a gold substrate by a variable thickness dielectric layer were predicted and found to be in excellent agreement with experiment for all three beam polarizations measured. The model calculation was then extended to other widely used thin-film systems on solid substrates and compared to experimental results measured in this work or already reported in the literature. The influence of the substrate and the beam geometry on measured SFG spectra from thin films is discussed in the context of the simulation results. The consistency of the simulation results with the present experimental observations and with previous experimental observations confirms the validity of the thickness interference simulation method. It is confidently anticipated that the present model calculation will be used to predict the SFG intensity and shape from many other thin-film systems by appropriately changing the parameters in the model.

ACKNOWLEDGMENTS

The work is supported by PRESTO, Japan Science and Technology Agency (JST), and a Grant-in-Aid for Exploratory Research (Grant No. 21655074) from MEXT.

[1] Y. Tong, Y. Zhao, N. Li, M. Osawa, P. B. Davies, and S. Ye, J. Chem. Phys. **133**, 034704 (2010).
[2] S. Ye, H. Noda, S. Morita, K. Uosaki, and M. Osawa, Langmuir **19**, 2238 (2003).
[3] S. Ye, H. Noda, T. Nishida, S. Morita, and M. Osawa, Langmuir **20**, 357 (2004).
[4] Y. Tong, N. Li, H. Liu, A. Ge, M. Osawa, and S. Ye, Angew. Chem., Int. Ed. **49**, 2319 (2010).
[5] J. Holman, P. B. Davies, and D. J. Neivandt, J. Phys. Chem. B **108**, 1396 (2004).
[6] J. Holman, P. B. Davies, T. Nishida, S. Ye, and D. J. Neivandt, J. Phys. Chem. B **109**, 18723 (2005).
[7] T. Nishida, C. M. Johnson, J. Holman, M. Osawa, P. B. Davies, and S. Ye, Phys. Rev. Lett. **96**, 077402 (2006).
[8] A. Lagutchev, S. A. Hambir, and D. D. Dlott, J. Phys. Chem. C **111**, 13645 (2007).
[9] S. Vitta, T. H. Metzger, S. S. Major, A. Dhanabalan, and S. S. Talwar, Langmuir **14**, 1799 (1998).
[10] C. D. Bain, E. B. Troughton, Y. T. Tao, J. Evall, G. M. Whitesides, and R. G. Nuzzo, J. Am. Chem. Soc. **111**, 321 (1989).
[11] The thicknesses shown here already includes the thicknesses of the bottom-most d-ODT monolayer and the top-most per-protonated arachidate monolayer.
[12] Y. S. Shon, R. Colorado, C. T. Williams, C. D. Bain, and T. R. Lee, Langmuir **16**, 541 (2000).
[13] H. P. Zhang, C. Romero, and S. Baldelli, J. Phys. Chem. B **109**, 15520 (2005).
[14] P. Guyot-Sionnest, J. H. Hunt, and Y. R. Shen, Phys. Rev. Lett. **59**, 1597 (1987).
[15] A. L. Harris, C. E. D. Chidsey, N. J. Levinos, and D. N. Loiacono, Chem. Phys. Lett. **141**, 350 (1987).
[16] S. Ye, S. Nihonyanagi, and K. Uosaki, Phys. Chem. Chem. Phys. **3**, 3463 (2001).
[17] L. J. Richter, T. P. Petralli-Mallow, and J. C. Stephenson, Opt. Lett. **23**, 1594 (1998).
[18] A. G. Lambert, D. J. Neivandt, A. M. Briggs, E. W. Usadi, and P. B. Davies, J. Phys. Chem. B **106**, 5461 (2002).
[19] S. J. McGall, P. B. Davies, and D. J. Neivandt, J. Phys. Chem. B **108**, 16030 (2004).
[20] H. Noguchi, M. Hiroshi, T. Tominaga, J. P. Gong, Y. Osada, and K. Uosaki, Phys. Chem. Chem. Phys. **10**, 4987 (2008).
[21] H. Rangwalla, A. D. Schwab, B. Yurdumakan, D. G. Yablon, M. S. Yeganeh, and A. Dhinojwala, Langmuir **20**, 8625 (2004).
[22] A. Opdahl, T. S. Koffas, E. Amitay-Sadovsky, J. Kim, and G. A. Somorjai, J. Phys.: Condens. Matter **16**, R659 (2004).
[23] G. P. Harp, H. Rangwalla, M. S. Yeganeh, and A. Dhinojwala, J. Am. Chem. Soc. **125**, 11283 (2003).
[24] S. Ye, S. Morita, G. F. Li, H. Noda, M. Tanaka, K. Uosaki, and M. Osawa, Macromolecules **36**, 5694 (2003).
[25] M. Oh-e, H. Yokoyama, and D. Kim, Phys. Rev. E **69**, 051705 (2004).
[26] M. B. Feller, W. Chen, and Y. R. Shen, Phys. Rev. A **43**, 6778 (1991).
[27] X. Wei, S. C. Hong, X. W. Zhuang, T. Goto, and Y. R. Shen, Phys. Rev. E **62**, 5160 (2000).
[28] C. Y. Chen, J. Wang, C. L. Loch, D. Ahn, and Z. Chen, J. Am. Chem. Soc. **126**, 1174 (2004).
[29] C. L. Loch, D. Ahn, C. Y. Chen, J. Wang, and Z. Chen, Langmuir **20**, 5467 (2004).
[30] D. Zhang, R. S. Ward, Y. R. Shen, and G. A. Somorjai, J. Phys. Chem. B **101**, 9060 (1997).
[31] Z. Chen, Y. R. Shen, and G. A. Somorjai, Annu. Rev. Phys. Chem. **53**, 437 (2002).
[32] X. Wei, X. W. Zhuang, S. C. Hong, T. Goto, and Y. R. Shen, Phys. Rev. Lett. **82**, 4256 (1999).
[33] A. Rao, H. Rangwalla, V. Varshney, and A. Dhinojwala, Langmuir **20**, 7183 (2004).
[34] F. Ding, Q. Zhong, M. R. Brindza, J. T. Fourkas, and R. A. Walker, Opt. Express **17**, 14665 (2009).
[35] R. N. Ward, P. B. Davies, and C. D. Bain, J. Phys. Chem. **97**, 7141 (1993).
[36] M. A. Hines, J. A. Todd, and P. Guyot-Sionnest, Langmuir **11**, 493 (1995).
[37] A. G. Lambert, D. J. Neivandt, A. M. Briggs, E. W. Usadi, and P. B. Davies, J. Phys. Chem. B **106**, 10693 (2002).
[38] C. D. Bain, P. B. Davies, T. H. Ong, R. N. Ward, and M. A. Brown, Surf. Interface Anal. **17**, 529 (1991).
[39] G. Q. Lu, A. Lagutchev, D. D. Dlott, and A. Wieckowski, Surf. Sci. **585**, 3 (2005).
[40] M. Himmelhaus, F. Eisert, M. Buck, and M. Grunze, J. Phys. Chem. B **104**, 576 (2000).
[41] Z. D. Schultz, M. E. Biggin, J. O. White, and A. A. Gewirth, Anal. Chem. **76**, 604 (2004).
[42] C. Romero and S. Baldelli, J. Phys. Chem. B **110**, 11936 (2006).
[43] W. Zhou, S. Ye, M. Abe, T. Nishida, K. Uosaki, M. Osawa, and Y. Sasaki, Chem.-Eur. J. **11**, 5040 (2005).
[44] P. Guyot-Sionnest, A. Tadjeddine, and A. Liebsch, Phys. Rev. Lett. **64**, 1678 (1990).